Atmospheric Environment Vol. 12, pp. 2439–2447.

0004–6981/78/1201–2439 $02.00/0

PLUME OPACITY RELATED TO PARTICLE MASS CONCENTRATION AND SIZE DISTRIBUTION

JOHN F. THIELKE and MICHAEL J. PILAT
Department of Civil Engineering,
University of Washington, Seattle, WA 98195, U.S.A.

(*First received* 29 *August* 1977 *and in final form* 28 *March* 1978)

Abstract – Simultaneous measurements of the in-stack light transmittance, particle mass concentration and particle size distribution were conducted on a hogged fuel boiler, a Kraft recovery furnace and a pulverized coal-fired boiler. The experimental data were utilized to evaluate a technique for predicting particulate mass concentration based on the particle characteristics. The predicted relationship between in-stack transmittance and particulate mass concentration was in good agreement with the experimental measurements for the hogged fuel boiler and the pulverized coal-fired boiler. The discrepancy noted in the predicted relationship for the Kraft recovery furnace may have been caused by measurement problems associated with low particulate mass concentrations or uncertainties in a value for the average particle density. An approach is presented for estimating the transmittance across a given light path based on the ratio of the specific volume to light extinction coefficient for monodisperse particle size increments. Figures are provided for determining this ratio for a wide range of particle sizes and refractive indices. The results of this study indicate the importance of using the actual particle size distribution for predicting the relationship between transmittance and mass concentration. An example problem is presented to illustrate the application of the calculation technique.

NOMENCLATURE

b	Light extinction coefficient (m^{-1})
b_n	Light extinction coefficient for the nth particle size increment (m^{-1})
f_n	Mass fraction of particles in the nth particle size increment
$f(r)$	Fractional particle size distribution by number
g_{n_i}	Particle mass fraction in the nth size increment from the ith process
I	Intensity of transmitted light
I_0	Intensity of incident light
K	Specific particle volume light extinction coefficient ratio ($cm^3\,m^{-2}$)
K_n	Monodisperse specific particle volume light extinction coefficient ratio characteristic of the nth particle size increment ($cm^3\,m^{-2}$)
L	Optical pathlength through aerosol (m)
Q_{ext}	Particle light extinction efficiency function
q_i	Gas flow rate in the ith exhaust duct ($m^3\,min^{-1}$)
r	Particle radius (m)
W	Aerosol mass concentration ($g\,m^{-3}$)
w_i	Mass concentration in the ith exhaust duct ($g\,m^{-3}$)
ρ	Particle density ($g\,cm^{-3}$)
ρ_n	Particle density characteristic of the nth size increment ($g\,m^{-3}$)
σ_g	Standard geometric deviation of lognormal distribution

I. INTRODUCTION

The relationship between plume opacity and aerosol properties has become increasingly important for the air pollution control engineer in recent years. Under most circumstances the attainment of acceptable emission levels must include consideration of plume opacity as well as particulate mass or concentration standards. Until recently, no techniques were available for relating aerosol properties to plume opacity other than reliance on previous experience. This experience, both in Europe and the U.S. has shown that fairly good agreement can be obtained between *in situ* opacity measurements and aerosol mass concentration for various sources including cement kilns and lignite-fired boilers (Beutner, 1974); a Kraft recovery furnace (Larssen *et al.*, 1972); a coal carbonization unit (Crocker, 1975); a catalytic regenerating unit, a sewage sludge incinerator, an asphaltic concrete plant, a secondary brass and lead smelter (Reisman *et al.*, 1974) and other source types. These correlations, however, have proven to be source specific and they must be obtained on a process-by-process basis.

The authors have been investigating the relationship between plume opacity and aerosol properties as part of a research program at the University of Washington initiated in 1969. The overall goal of this work has been to study the use of optical transmissometry as a continuous monitor of particle mass emissions. The current study focuses on the experimental validation of a theoretical relationship between plume opacity and particulate mass concentration developed from Mie theory (Pilat and Ensor, 1970). In order to assess the validity of the mass concentration–opacity relationship, simultaneous measurements of light transmittance, particle mass concentration and particle size distribution were obtained from a variety of sources and the results were compared with theoretical predictions. In particular, the earlier work has been extended to include consideration of particle size

distributions which deviate from the log-normal model and the influence this variation will have on the optical properties of the aerosol. The results of this investigation suggest that such deviations are important in terms of using opacity measurements to predict particulate mass concentrations.

II. IN-STACK LIGHT TRANSMITTANCE AND MASS CONCENTRATION RELATIONSHIPS

The light extinction property of an aerosol as measured in a stack or duct is given by the Bouguer Law (Beer–Lambert Law)

$$\frac{I}{I_0} = e^{-bL} \tag{1}$$

where I is the intensity of the transmitted light, I_0 is the incident light intensity, L is the optical path length through the aerosol and b is the extinction coefficient (m^{-1}). Based on earlier studies (Pilat and Ensor, 1970), the aerosol mass concentration, W, can be related to optical transmittance in a modified form of the Bouguer Law such that

$$\ln\frac{I}{I_0} = -\frac{WL}{K\rho}, \tag{2}$$

where ρ is the average particle density and K is the ratio of the specific particle volume to light extinction coefficient. The parameter K can be calculated from

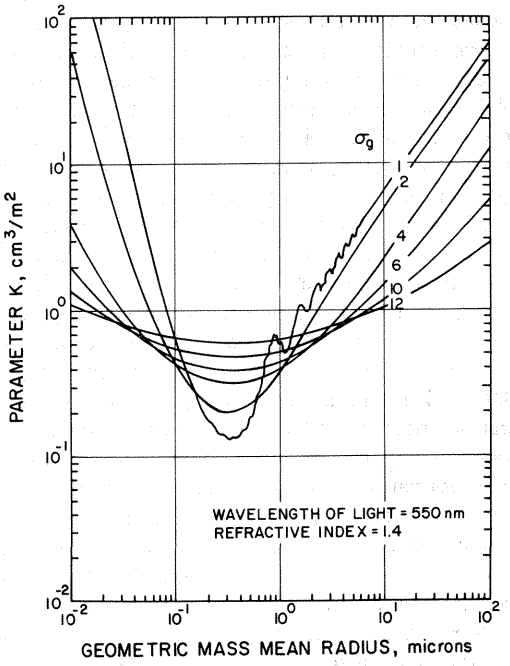

Fig. 1. The parameter K as a function of the log-normal particle size distribution parameters.

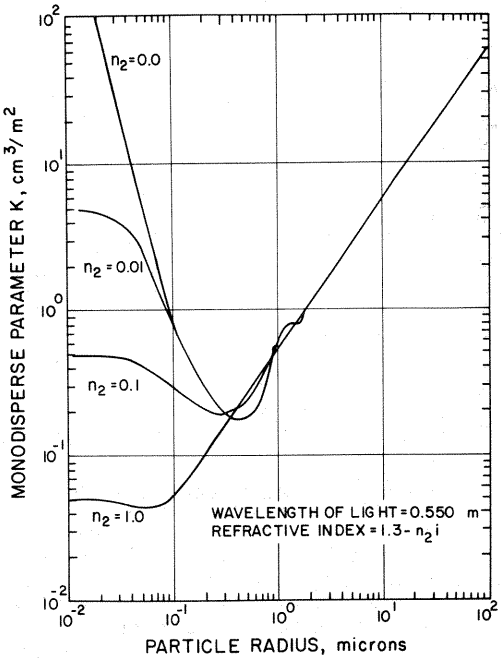

Fig. 2. Monodisperse parameter K as a function of particle size for a scattering component of 1.3 and various absorbing components.

Mie theory by means of the equation (Pilat and Ensor, 1970)

$$K = \frac{\frac{4}{3}\int_{r_1}^{r_2} r^3 f(r)\,dr}{\int_{r_1}^{r_2} Q_{ext} r^2 f(r)\,dr} \tag{3}$$

given the particle fractional frequency, $f(r)$, and the particle light extinction efficiency factor, Q_{ext}, which is a function of the wavelength of the indicent light, the particle size and refractive index of the material. The parameter K may vary considerably as a function of particle size distribution parameters and the refractive index at a given wavelength. For poly-disperse systems with log-normal distributions, however, the parameter K tends to be fairly constant over the range of particle diameters from 0.2 to 10 μm as indicated in Fig. 1. This has led to the suggestion (Larssen *et al.*, 1972) that for such distributions the parameter K is well defined and that good correlations between opacity and particulate mass concentration are likely.

Difficulties arise, however, when the size distribution data do not fit the log-normal model (Jarman and deTurville, 1970) or when particle density and refractive index are a function of particle size. In this case, it is necessary to use Equation 3 to calculate a value for K based on the actual size distribution data and aerosol properties. Recalling the form of the Bouguer Law given in Equation 1, it can be reasoned that each component of the aerosol size distribution

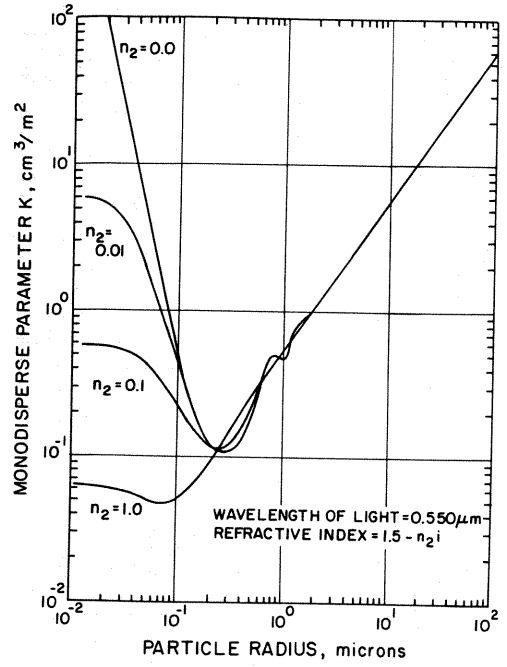

Fig. 3. Monodisperse parameter K as a function of particle size for a scattering component of 1.5 and various absorbing components.

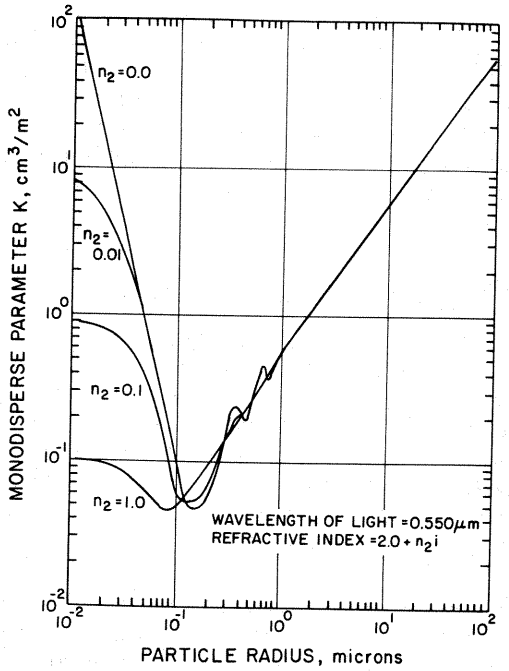

Fig. 5. Monodisperse parameter K as a function of particle size for a scattering component of 2.0 and various absorbing components.

scatters and/or absorbs light independently such that

$$\ln\frac{I}{I_0} = -L(b_1 + b_2 + \ldots b_n) \qquad (4)$$

where b_n is the extinction coefficient for the nth size increment in the overall particle size distribution.

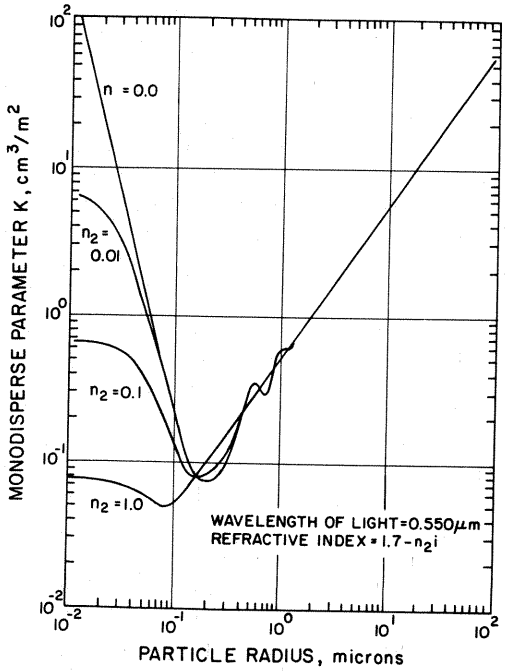

Fig. 4. Monodisperse parameter K as a function of particle size for a scattering component of 1.7 and various absorbing components.

Based on the definition of K. Equation 2 can be put in a form similar to (4) giving

$$\ln\frac{I}{I_0} = -LW\left(\frac{f_1}{K_1\rho_1} + \frac{f_2}{K_2\rho_2} \ldots + \frac{f_n}{K_n\rho_n}\right) \qquad (5)$$

where f_n is the fraction of total mass, ρ_n is the particle density, and K_n is the monodisperse specific volume to extinction coefficient ratio characteristic of the nth particle size increment. The value for f_n can be determined from the cumulative particle size distribution plotted on log-probability axes and K_n is obtained using Equation 3 between the limits r_1 and r_2 which define the size increments. When the size increment is small, the value of K can be determined on the basis of the monodisperse particle radius characterized by the midpoint of the interval. Calculated values of K for monodisperse particles as a function of particle radius and refractive index are shown in Figs. 2–5 for scattering components of the refractive index of 1.3, 1.5, 1.7, and 2.0 respectively. In each figure, K has been determined over the particle size range of 0.01–100 μm for absorptive components of the refractive index of 0.0, 0.01, 0.10, and 1.0 at 550 nm. The value of K is insensitive to changes in the refractive index for particle radii greater than 0.5 μm. For smaller particle sizes, however, both components of the refractive index are important. Note that the calculated curves have been smoothed somewhat to facilitate computational use.

The use of Equation 5, together with the figures relating K to particle size for various refractive indices at 550 nm can be used to characterize the relationship

of light transmittance to particulate mass concentration for particle distributions which do not fit the log-normal model. In addition, since K is evaluated incrementally over the size distribution, it is possible to account for differences in refractive indices that may occur as a function of particle size. In particular, this is important when two different process streams may be discharged to a common stack or when the particulate material is emitted from a complex chemical or combustion process in which different mechanisms of particle generation and transformation exit in parallel (Jarman and de Turville, 1970).

The procedure for determining the relationship between particle mass concentration and light transmittance for any size distribution is to subdivide the size distribution into a number of intervals and to determine the fraction f_n, of the total mass in each increment. The number of increments selected should be sufficient to give good resolution in the particle size range of 0.2 to 2 μm in diameter. The characteristic particle radius in each increment and the assumed or measured refractive index at a given wavelength (550 nm), are used to determine a value of K_n for each interval by relying on the appropriate figure. The overall relationship between particulate mass concentration and light transmittance can then be calculated by summing the individual contributions as indicated by Equation 5 if the average particle density in each interval, ρ_n, is known or estimated. An example calculation is provided in the Appendix.

III. EXPERIMENTAL MEASUREMENTS

A. Apparatus and sampling techniques

Simultaneous measurements of the particulate size distribution, in-stack transmittance and mass concentration have been conducted at various emission sources. These sources include a hogged fuel boiler, a Kraft recovery furnace and a pulverized coal-fired boiler. The apparatus for these tests consists of a transmissometer, an in-stack cascade impactor and a mass concentration sampling train.

Size distributions. The particle size distributions were measured with a University of Washington Source Test Cascade Impactor (Pilat *et al.*, 1970). The cascade impactor consists of a series of multi-jet stages followed by a glass fiber filter. The impactors used in this study are specifically designed for source testing and separate the particles into size classes characterized by the aerodynamic diameter and density of the particle. Particle size distributions from the hogged fuel boiler and the Kraft recovery furnace were measured with a Mark 3 impactor over the size range of 0.3 to 30 μm in diameter. Sampling on the pulverized coal-fired boiler was conducted with a Mark 4 impactor system described by Pilat *et al.* (1977) capable of sizing particles from 0.05 to 30 μm. Because a filter is used following the impactor, the sum of the particle mass on each collection stage and the mass on the filter provides a value which can be used to calculate the mass concentration as well as provide size distribution data.

Opacity measurements. The light transmittance was measured with a Lear Seigler RM-Series 4 portable in-stack transmissometer (Beutner, 1974). The wave length of light used in this instrument is centered at 550 nanometers and is passed over a folded light path in a probe which is inserted into the stack. Output from the instrument consists of linear values of opacity and optical density. For the tests involving a Kraft recovery furnace, a permanently mounted transmissometer with a path length of 8.5 m was utilized to measure transmittance in addition to the smaller, portable unit.

Mass concentration. The particle mass concentration for tests on the hogged fuel boiler was determined using an alundum thimble holder with a coarse porosity alundum filter lined with glass wool. The alundum thimble was followed by a 47 mm dia glass fiber filter to collect any particles not collected by the alundum filter. EPA Method 5 was used to measure mass concentration for a portion of the tests on the pulverized coal-fired boiler. For tests in which neither the alundum thimble or the Method 5 equipment were used, the total mass catch in the cascade impactor was used to estimate the mass concentration. A comparison between the cascade impactor and the other methods yielded a good agreement.

B. Results

Kraft recovery furnace. Simultaneous measurements of in-stack transmittance, particle size distribution and particle mass concentration were made downstream of a Kraft recovery furnace equipped with an electrostatic precipitator. The power to various fields of the precipitator was shut off to provide a range of opacity and mass concentration values. The characteristic particle size distributions obtained for each operating condition are presented in Fig. 6 as a percent smaller by weight versus particle diameter on log probability axes. As shown, the actual size distribution cannot be well represented by a log-normal distribution (which would plot as a straight line on the graph). The differential particle size distributions shown in Fig. 7 indicates bimodal characteristics for the Kraft recovery furnace emissions. When fields of the precipitator are turned off, the mass mean diameter increases and the overall distribution tends to become less polydisperse as indicated by the overall shape of the distributions.

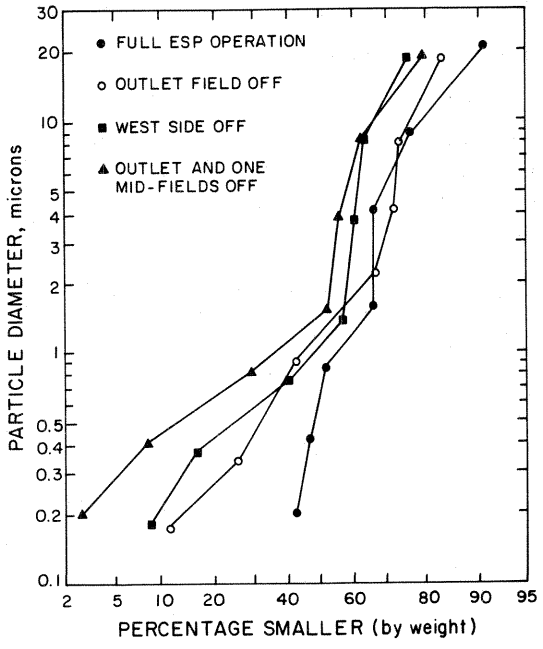

Fig. 6. Average particle size distributions for Kraft recovery furnace.

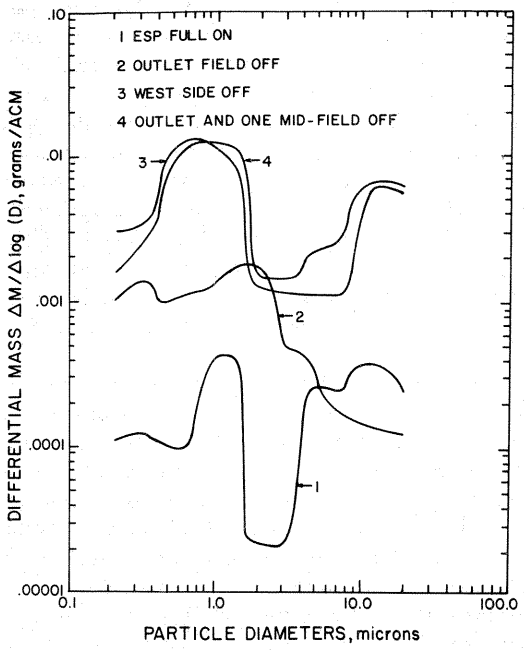

Fig. 7. Differential particle size distributions for Kraft recovery furnace.

The experimental relationship between in-stack transmittance and mass concentration for the Kraft recovery furnace is shown in Fig. 8 together with the calculated values using the parameter K based on the actual measured and the log-normal approximation to the particle size distribution. Previous work (Bosch, 1969) has shown the composition of Kraft recovery furnace emissions are approx 76% Na_2SO_4 and 18% NaCl by weight. The average density of the particles was assumed to be 2.6 g cm^{-3} and the refractive index was taken to be (1.5–0.01) based on the bulk properties for Na_2SO_4.

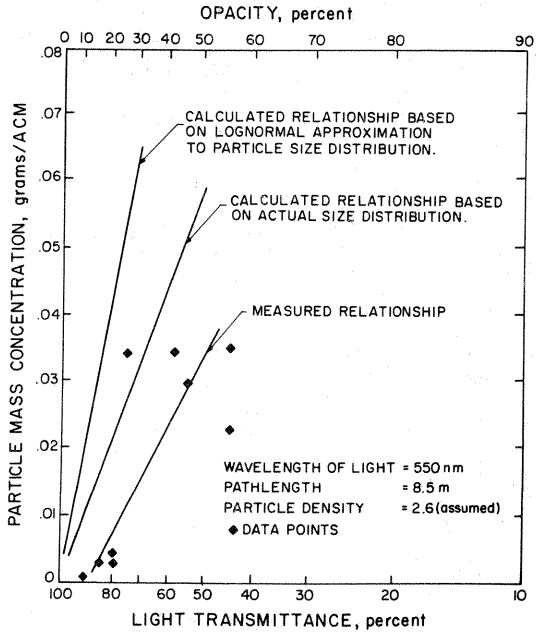

Fig. 8. Relationship between particle mass concentration and light transmittance for Kraft recovery furnace.

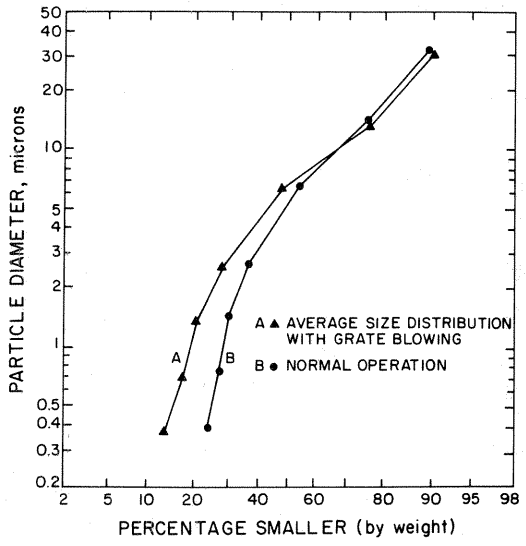

Fig. 9. Average particle size distributions for a hogged fuel boiler.

Hogged fuel boiler. In-stack transmittance, particulate size distributions and particle mass concentrations were measured downstream of the cyclone collectors on a hogged fuel boiler burning a mixture of bark, shavings and sawdust. Average particle size distributions were obtained for normal boiler operation and during grate blowing as illustrated in Fig. 9. The grate blowing resulted in a smaller percentage of smaller particles in the stack and slightly larger mass mean diameter.

The in-stack transmittance and mass concentration data for the hogged fuel boiler are presented in Fig. 10. The calculated relationship is also shown based on the actual and

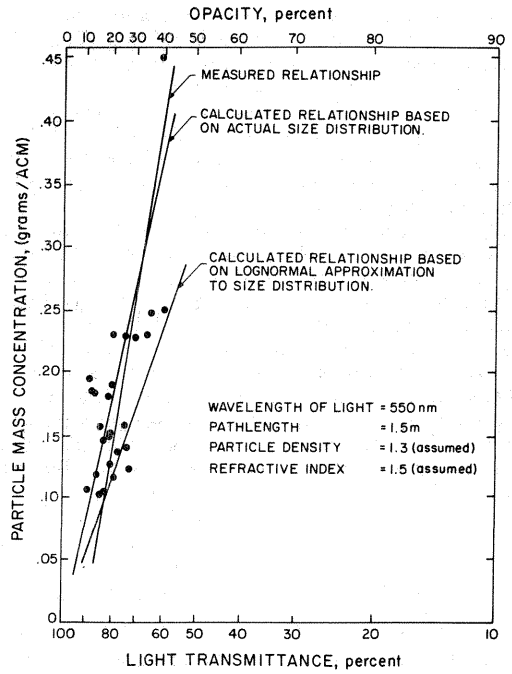

Fig. 10. Relationship between particle mass concentration and light transmittance for a hogged fuel boiler.

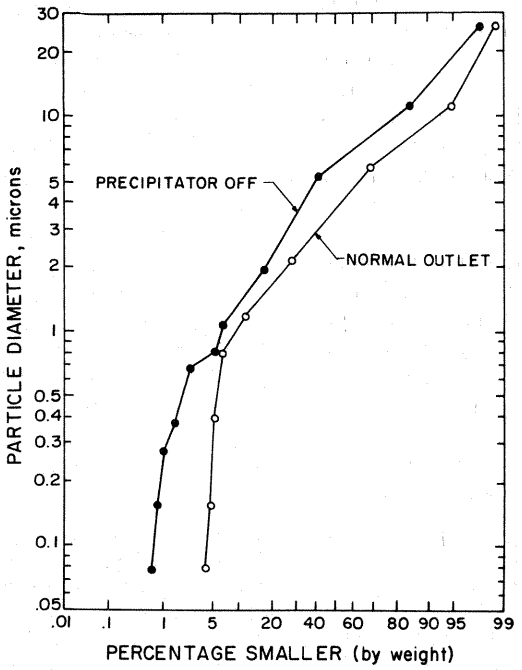

Fig. 11. Average particle size distributions for pulverized coal-fired boiler.

log-normal approximation to the particle size distribution. The particulate material collected from the hogged fuel boiler was extremely non-homogeneous and it was difficult to measure or estimate a value for the refractive index. A microscopic examination revealed multi-colored particles ranging from white crystalline material to amorphous black particles. The refractive index of the particles was taken to be 1.5 and the particle density was assumed to be equal to $1.3\,g\,cm^{-3}$ based on data reported for wood smoke (Foster, 1959).

Pulverized coal-fired boiler. Size distribution data for a pulverized coal-fired boiler are shown in Fig. 11. The boiler utilized western coal with a dry analysis of 12,847 BTU per pound, 10.3% ash and 0.57% sulfur. High opacity levels were generated by turning off the electrostatic precipitator. The particle size distributions shown in Fig. 11 indicate that the average mass mean diameter increases when the electrostatic precipitator is turned off as compared with the normal operating conditions.

Light transmittance and mass concentration data are presented in Fig. 12 including the calculated relationship based on the actual and log-normal size distribution. A microscopic examination of cascade impactor collection stages revealed a substantial portion of the material was glass-like in character. In addition, the collected material for the smaller particle sizes appeared to be darker in appearance. The refractive index of the material was assumed, however, to be constant over the size spectrum and was assumed equal to 1.5 based on data for SiO_2. A particle density of 2.3 was assumed based on a value reported for fly ash (Noll and Davis, 1976).

IV. DISCUSSION

Comparison of experimental and calculated results

In general, good agreement was obtained between the measured particle mass concentration/light transmittance relationships and the calculated relationships based on the actual particle size distribution data. A discrepancy can be noted, however, for the Kraft recovery furnace results. This discrepancy may have been caused by experimental error due to extremely low mass concentration values or because the assumed particle density of $2.6\,g\,cm^{-3}$ based on the bulk properties of Na_2SO_4 may not reflect the apparent density of the material in particulate form. Previous studies (Larssen *et al.*, 1972) showed good agreement between experimental and calculated data for Kraft recovery furnace emissions which may indicate experimental error attributable to the low particulate mass concentration conditions characteristic of the furnace tested in this study.

The calculated relationship between the particle mass concentration and light transmittance appears to be in better agreement using the actual size distribution compared to the log-normal model. Recalling that the optically active portion of the size distribution is in the range of particle diameters from 0.2 to 2.0 μm for nonabsorbing particles, an examination of the measured size distribution reveals that a log-normal approximation to the actual data will not adequately represent the size distribution in this region. For the case of the pulverized coal-fired boiler and the hogged fuel boiler, the log-normal approximation tends to overestimate the particle mass in the optically active region due to the downward concave shape of the size distribution. This is reflected in the calculated relationship between the particle mass and light transmittance based on the log-normal approximation which indicates a lower mass concentration than the measured value for a given value of transmittance. Conversely, the particle size distribution for the Kraft recovery furnace is slightly concave upwards and a log-normal approximation underestimates the percentage

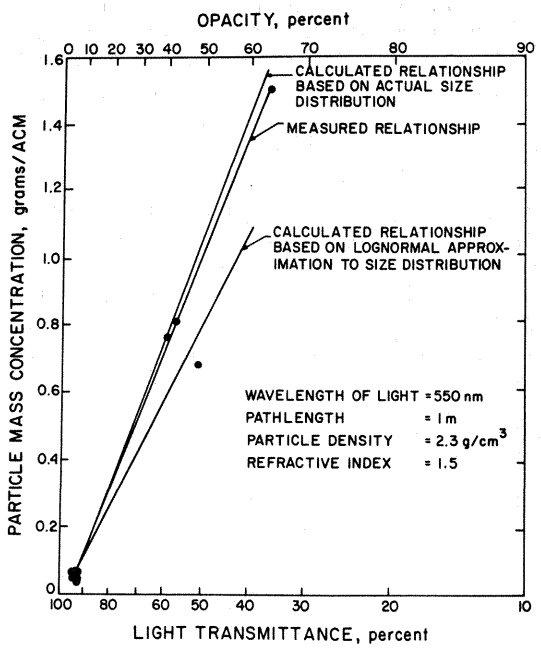

Fig. 12. Relationship between particle mass concentration and light transmittance for pulverized coal-fired boiler.

of mass in the 0.2 to 2 μm dia size range. As a result, the calculated relationship based on the log-normal approximation will predict higher mass concentrations than measured for a given value of light transmittance. Based on this analysis, it can be seen that the actual size distribution is important in determining a calculated value for the K parameter such that the particle mass concentration can be related to light transmittance. The utilization of Equation 5 permits such an evaluation for cases in which the particle size distribution cannot adequately be approximated by a log-normal distribution.

Relative to the results reported above, certain measurement difficulties are often encountered for low mass concentration and high light transmittance conditions. The relative error in the logarithm of the light transmittance near unity $[(I/I_0) \sim 1.0]$ becomes very large due to measurement limitations, particularly if a limited pathlength is used. This implies that it is generally not possible to develop a statistically valid experimental relationship between particle mass concentration and light transmittance if data are limited to high transmittance conditions. As a result, it is generally necessary to modify the performance of the control equipment or the process in order to generate opacity levels that can provide a valid statistical relationship between in-stack light transmittance and particle mass concentration. In practice, however, simultaneous changes in the particle size distribution, the refractive index, and particle density may occur which do not correspond to the manner in which the relationship between mass concentration and light transmittance was obtained experimentally. For example, the power to various sections of an electrostatic precipitator can be reduced or turned off to create higher mass loadings and opacity conditions downstream. These data are usually plotted to provide an experimental relationship between opacity and mass concentration. This relationship may not be valid if particle characteristics change as a result of process conditions or as other factors associated with the control device efficiency come into play. Thus, it becomes a matter of some importance to characterize the mass concentration vs light transmittance relationship under conditions that are expected normally to occur. Since the primary use of plume opacity standards in the U.S. (as interpreted by the EPA) is to insure that control systems, required by mass or concentration emission standards, are properly operated and maintained at all times (Goodwin, 1977), it would appear that control device modification to generate a mass concentration-light transmittance relationship is a valid procedure if care is taken to approximate as closely as possible the conditions encountered under normal operation and monitoring.

CONCLUSIONS

Simultaneous measurements of the particle mass concentration, particle size distribution and in-stack light transmittance have served to examine experimentally the relationship between light transmittance and particulate mass concentration. Theoretical calculations of particulate mass concentration based on size distribution parameters, particle refractive index and the wave-lengths of light were in good agreement with experimental data. In particular, a method has been presented for characterizing the relationship between particulate mass concentration and light transmittance when the particle size distribution deviates from the log-normal model. This method appears to offer considerable utility for the air pollution engineers involved in the design and selection of air pollution control equipment. The results of this work also suggest that when properly applied and interpreted, transmissometry offers a continuous method for measuring particle mass concentrations from certain emission sources.

Acknowledgements – The authors appreciate the cooperation and assistance of Ralph Buchanan and James Pearson of the University of Washington Physical Plant, and William Conner and his staff, EPA Division of Chemistry and Physics, for valuable comments and suggestions regarding experimental phases of this work. The valuable assistance of David Mummey in the coal-fired boiler sampling is also appreciated. Source testing and data analysis for the hogged fuel boiler and Kraft recovery furnace were conducted by David Lutrick with assistance provided by Anil Prem.

This work was supported under EPA Grant No. R803897-02.

REFERENCES

Beutner H. P. (1974) Measurement of opacity and particulate emissions with an in-stack transmissometer. *J. Air Pollut. Control Ass.* **24,** 865–871.

Bosch J. C., Pilat M. J. and Hrutfiord B. F. (1971) Size distribution of aerosols emitted from a Kraft recovery furnace. *Tappi*, **54,** 1871–1875.

Crocker B. B. (1975) Monitoring particulate emissions. *Chem. Engng Progr.* **71,** 83–89.

EPA (1971) Standards of Performance for New Stationary Sources. *Federal Register*, **36,** No. 247, 24876–95.

Foster W. W. (1959) Attenuation of light by woodsmoke. *Br. J. appl. Phys.* **10,** 416–420.

Goodwin D. R. (1977) Opacity, a federal view. *Envir. Sci. Techn.* **11,** 10–11.

Jarman R. T. and de Turville C. M. (1970) Plume opacity and particle mass concentration. *Atmospheric Environment*, **5,** 589–590.

Larssen S., Ensor D. S. and Pilat M. J. (1972) Relationship of plume opacity to the properties of particles emitted from Kraft recovery furnaces. *Tappi*, **55,** 88–92.

Noll K. E. and Davis W. T. (1976) *Power Generation*, Ann Arbor Science, New York.

Pilat M. J. and Ensor D. S. (1970) Plume opacity and particulate mass concentration. *Atmospheric Environment* **4,** 163–173.

Pilat M. J., Ensor D. S. and Bosch J. C. (1970) Source test cascade impactor, *Atmospheric Environment* **4,** 671–675.

Pilat M. J., Powell E. B. and Carr R. C. (1977) Submicron Particle Sizing with UW Mark 4 Cascade Impactor, Paper 77-35.2 presented at the 70*th Annl Mtng Air Pollut. Control Ass.*, Toronto, Ontario, Canada, June 20–24.

Reisman E., Gerber W. D. and Potter N. D. (1974) In-stack Transmissometer Measurement of Particulate Opacity and Mass Concentration. Environmental Protection Agency, Office of Research and Development, Report EAP-640/2-74-120.

APPENDIX

Example calculation

The following example problem is presented to illustrate the technique for predicting in-stack light transmittance (opacity) for a complicated source.

Assume two processes, labeled *A* and *B*, discharge to a common stack-one meter in diameter. The particle size distributions for each process are known and given in Figure A1. The particulate characteristics are summarized in Table 1.

For convenience, the particle size distributions have been subdivided into seven intervals as listed in Table 2. The mean particle radius characteristic of each interval is used, together with the particle refractive index at 550 nm to determine the parameter K for each size class as shown in Table 2 for both size distributions.

The basic equation relating light transmittance and mass concentration is expressed similarly to Equation 5 presented earlier

$$\ln\frac{I}{I_0} = -LW\sum\frac{fn}{K_n\rho_n}, \tag{6}$$

where L is given as 1 m and W is the mass concentration in the stack resulting from the combination of the two exhaust flows. W is determined by mass balance such that

$$W = \frac{\sum w_i q_i}{\sum q_i} \tag{7}$$

where

W = combined mass concentration in stack ($g\,m^{-3}$)
w_i = mass concentration in individual exhausts ($g\,m^3$)
q_i = gas flow rate in each exhaust duct ($m^3\,min^{-1}$).

Table 1. Particle characteristics for example problem

Particle characteristic	Process A	Process B
Particle density, $g\,cm^{-3}$	1.0	3.0
Particle refractive index (at 550 nm)	1.5	2.0–0.1i
Particulate mass concentration ($g\,m^{-3}$)	0.12	0.06
Gas flow rate, ($m^3\,min^{-1}$)	100	200

Using the values given in Table 1, the mass concentration in the stack is

$$W = \frac{(0.12)(100)+(0.06)(200)}{(100+200)} = 0.08\ g\,m^{-3}. \tag{8}$$

The fraction of mass in the nth increment, f_n, is determined using the size distribution and particle mass concentration data such that

$$f_n = \frac{\text{mass concentration in the } n\text{th size interval}}{\text{total mass concentration}}. \tag{9}$$

Because the particle characteristics are different for each process discharge, the size intervals in each distribution must be evaluated separately rather than summing the mass in each size increment. The mass concentration in the nth size interval, W_n, is given by

$$W_n = \frac{g_{n_i} w_i q_i}{\sum q_i} \tag{10}$$

where g_{n_i} is the mass fraction in the nth particle size increment from the ith distribution. From the above, the fraction of mass

Table 2. Determination of f_n and K_n values for example problem

Particle diameter size interval (μm)	Mean particle radius (μm)	Mass fractions in each size interval		Mass fractions in combined gas flow		Parameter $K_n\left(\frac{cm^3}{m^2}\right)$		$\frac{f_n}{K_n\rho_n}\left(\frac{m^2}{g}\right)$	
		Process A g_A	Process B g_B	Process A f_{n_A}	Process B f_{n_B}	Process A[(1)]	Process B[(2)]	Process A[(3)]	Process B[(4)]
< 0.1	0.05	0.04	0.05	0.02	0.025	7.0	0.45	0.00286	0.01852
0.1 – 0.27	0.09	0.07	0.13	0.035	0.065	0.6	0.09	0.05833	0.024074
0.27– 0.65	0.20	0.11	0.20	0.055	0.10	0.1	0.06	0.55	0.05556
0.65– 1.6	0.50	0.34	0.24	0.17	0.12	0.2	0.27	0.85	0.09877
1.6 – 4.0	1.25	0.37	0.20	0.185	0.10	0.7	0.7	0.26429	0.04524
4.0 –10.0	3.0	0.07	0.13	0.035	0.065	1.8	1.8	0.01944	0.01204
> 10.0	10.0	0.0	0.05	0.0	0.025	7.0	7.0	0.0	0.00119
	$\sum$ =	1.0	1.0				$\sum$ =	1.745	0.972

$\sum = 1.0$

$\sum \frac{f_n}{K_n\rho_n} = 2.717\left(\frac{m^2}{g}\right)$

Notes:
(1) Refractive index = 1.5 at 550 nm.
(2) Refractive index = 2.0–0.1i at 55 nm.
(3) Particle density = 1.0 $g\,cm^{-3}$.
(4) Particle density = 3.0 $g\,cm^{-3}$.

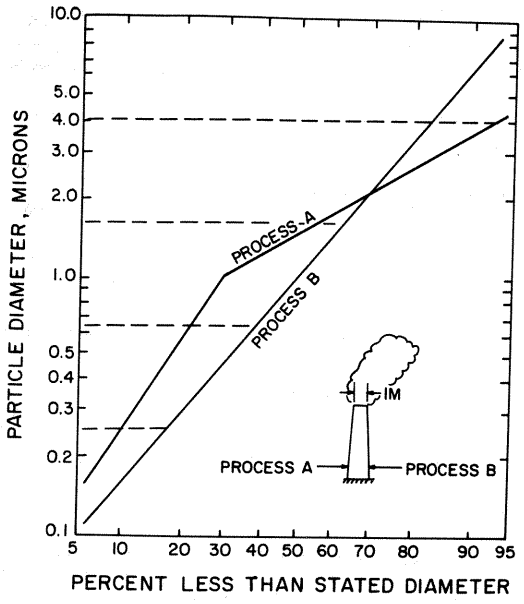

Fig. A1. Particle size distributions for example problem.

in each increment from each particle size distribution is

$$f_{n_i} = \frac{g_{n_i} w_i q_i}{\sum w_i q_i}. \tag{11}$$

Equation 11 was used to calculate the mass fractions in the combined gas flow for the particle size increments from each size distribution as shown in Table 2.

As shown in Table 2, the term $f_n/(K_n \rho_n)$ has been evaluated for each interval of the individual particle size distributions. Summing the individual contributions and substituting the appropriate values into Equation 6 yields an estimate of the transmittance across the stack such that

$$\ln\left(\frac{I}{I_0}\right) = (-1\text{m})\left(0.08\frac{g}{\text{m}^3}\right)\left(2{,}717\frac{\text{m}^2}{g}\right) = -0.217$$

or

$$\left(\frac{I}{I_0}\right) = 0.81.$$

The predicted opacity at the stack outlet is given by

$$\text{Opacity} = 1 - \left(\frac{I}{I_0}\right) = 0.19\ (19\%).$$